

# A microfabricated porous collagen-based scaffold as prototype for skin substitutes

Curtis D. Chin · Krishn Khanna · Samuel K. Sia

© Springer Science + Business Media, LLC 2007

**Abstract** An important element of artificial skin is a tissue scaffold that allows for fast host regeneration. We present a microfabrication strategy, based on gelling collagen-based components inside a microfluidic device, that produces well-controlled pore sizes inside the scaffold. This strategy can produce finely patterned tissue scaffolds of clinically relevant dimensions suitable for surgical handling. Compared to porous collagen-based sponges produced by lyophilization, microfabricated tissue scaffolds preserve the fibrous structure and ligand density of natural occurring collagen. A fibroblast migration assay revealed fast cellular migration through the pores, which is desired for rapid tissue ingrowth. Finally, we also demonstrate a strategy to use this microfabrication technique to build anatomically accurate, multi-component skin substitutes in a cost-effective manner.

**Keywords** Collagen · Skin · Microfabrication · Scaffold · Pore size

## 1 Introduction

This paper presents a microfabricated collagen-based scaffold as a structural alternative to conventional porous collagen sponges for skin substitutes. We outline a microreactor method that can produce a finely patterned scaffold—over clinically relevant size scales—sufficiently

robust for routine handling. This microfabrication approach produces pores of dimensions conducive to host tissue ingrowth while preserving the fibrous structure and ligand density of natural collagen; it also forms a basis for engineering anatomically complex skin substitutes made of many cellular and extracellular components.

Tissue-engineered skin is an important treatment option for acute injuries (such as burns) and chronic skin wounds (including cutaneous ulcers and congenital anomalies such as giant nevus) (Schulz et al. 2000; Boyce and Warden 2002; Jones et al. 2002; Supp and Boyce 2005; MacNeil 2007). By reducing or eliminating the donor site area that is needed for autologous split-thickness grafts, it makes skin-replacement procedures available to patients contraindicated for autologous grafts (such as patients with over 60% of total body surface area burned, young and elderly patients, and patients with smoke inhalation injuries) and decreases the patients' risk of infection and sepsis (especially at the thin dermis at the donor site; Schulz et al. 2000; Jones et al. 2002; MacNeil 2007). In addition, the use of skin substitutes reduces mortality and morbidity from scarring (both the donor and treatment sites), patients' burden of pain, cosmetic changes in pigmentation, and the total number of surgical procedures and hospitalization time (Boyce and Warden 2002; Supp and Boyce 2005). Although current artificial skin products (including cell-free scaffolds such as Integra and Alloderm, and cell-seeded materials such as Epicel, Dermagraft, Apligraf, Permaderm, and OrCel that serve to replace the dermis and/or the epidermis [Bell et al. 1979, 1981; Burke et al. 1981; Jaksic and Burke 1987; Wilkins et al. 1994; Waymack et al. 2000; Jones et al. 2002; MacNeil 2007]) have demonstrated success, there is strong clinical interest in new cost-effective methods that can produce scaffolds containing a

---

C. D. Chin · K. Khanna · S. K. Sia (✉)  
Department of Biomedical Engineering, Columbia University,  
351 Engineering Terrace, 1210 Amsterdam Ave,  
New York, NY 10027, USA  
e-mail: ss2735@columbia.edu

larger number of cellular and extracellular components (Jones et al. 2002; MacNeil 2007).

Microfabrication is a promising technique for generating high-precision skin-substitute scaffolds and for engineering multi-component structures (containing extracellular matrices such as collagen and basal lamina, and cells such as fibroblasts, keratinocytes, melanocytes, and endothelial cells). The capability of microfabrication methods and the structural characteristics of artificial skin are congruent: current microfabrication techniques can produce structures with lateral resolutions of tens of microns and thicknesses of hundreds of microns, which fit the dimensions of skin substitutes (Schulz et al. 2000; Boyce and Warden 2002; Jones et al. 2002; Supp and Boyce 2005). For example, laser machining was used to control the topography of the basal lamina (Pins et al. 2000; Downing et al. 2005), and micromolding techniques (such as replica molding, microtransfer molding, and micromolding in capillaries or MIMIC; Tang et al. 2003, 2004), layer-by-layer deposition (Tan and Desai 2004, 2005), and controlled etching methods produced patterns in scaffolds containing collagen (the predominant extracellular matrix in the dermal layer).

In this study, we use a microfabricated bioreactor to produce a centimeter-sized collagen-based scaffold whose porous features are well-controlled. Control over porous features is clinically important: for example, Yannas and colleagues discovered that to achieve minimal scarring in patients upon wound closure, the porous features of Integra (an acellular porous sponge that contains cross-linked collagen and chondroitin-6-sulfate [Balasubramani et al. 2001; Morgan et al. 2004]) must be tuned to an average diameter of 20 to 125  $\mu\text{m}$  to have sufficient ligand density for cell migration and at the same time be sufficiently porous for rapid ingrowth of host fibroblasts and endothelial cells (Yannas et al. 1989). Both scaffold porosity and composition affect ligand density by defining, respectively, the total surface of the structure exposed to cells and the surface density of ligands; cell attachment and viability are primarily influenced by scaffold specific area in collagen-glycosaminoglycan (collagen-GAG) sponges (O'Brien et al. 2005). Although freeze-drying yields the best control (compared to precipitation and critical point drying) over the rates of ice nucleation and crystal growth (Dagalakis et al. 1980; Yannas and Burke 1980; Yannas et al. 1980; Morgan et al. 2004; O'Brien et al. 2005), the precision in pore size and void fraction of collagen sponges remains below the capability of microfabrication techniques. In a second step, we also investigate the potential of the microfabrication methods to build, in a step-wise manner, epidermal and dermal substitutes that contain multiple cellular and extracellular components.

## 2 Materials and methods

### 2.1 Design and fabrication of microfluidic bioreactor

We designed nine skin scaffolds with cylindrical posts spanning void fractions of 20% to 60% and mean pore size of 70 to 120  $\mu\text{m}$ . We first generated a high-resolution photomask using computer-aided design and a commercial printing service (20,000 dpi from CAD/Art Services, Inc., Bandon, OR). Our microreactor design consisted of a center channel with a grid of posts spanning 11 mm long and 6 mm wide, and two tapered ends flanking either side of the channel for reagent delivery. The tapered ends also minimized bubble formation in the chamber.

Next, we used standard soft lithography to fabricate the microfluidic reactor (Sia and Whitesides 2003). Briefly, we spin-coated a 165- $\mu\text{m}$  layer of epoxy-based photoresist SU-8 2050 (MicroChem, Newton MA) onto a Si wafer (Silicon Sense, Nashua NH), exposed it to 365-nm light for 100 s through the photomask using a Karl Suss MJB3 contact mask aligner (Garching, Germany) and developed the features with propylene glycol monomethyl ether acetate (Sigma-Aldrich, St. Louis MO). After replica molding the masters with polydimethylsiloxane (PDMS) (Sylgard 184 Silicone Elastomer Kit, Dow Corning, Midland MI), we punched holes through the PDMS molds for inlets and outlets, treated them with bovine serum albumin (1% w/v in PBS) (Sigma-Aldrich, St. Louis MO), and conformally sealed them to a glass coverslip (Fisher Scientific, Pittsburgh PA) or thin PDMS membrane.

### 2.2 Fabrication of collagen-GAG scaffold

At 4°C, we mixed collagen rat tail type I (BD Biosciences, Bedford MA) with chondroitin-6-sulfate from shark cartilage (Sigma-Aldrich, St. Louis, MO), and neutralized the mixture with NaOH to pH 7.4 to yield a final gel concentration of 4 mg/mL collagen with 0.8 mg/mL  $\text{Ch}_6\text{SO}_4$  (procedure adapted from [Hanthamrongwit et al. 1996; Osborne et al. 1997]). We immediately injected the collagen-GAG mixture into the microfluidic reactor, and then gelled the mixture *in situ* by incubating it at 37°C for 1 h. We then dehydrated the gels by incubating it at 37°C for one day or until the gel completely dehydrated. By allowing the collagen structure to collapse, we could carefully peel the PDMS mold off the collagen-GAG scaffold. Attempts to peel off the collagen-GAG scaffold prior to complete dehydration led to poor fidelity of features. To handle the thin porous collagen membrane, we used tweezers to manipulate the scaffold on a thin PDMS membrane as backing. For assembly of multi-component structures and cell migration studies, we

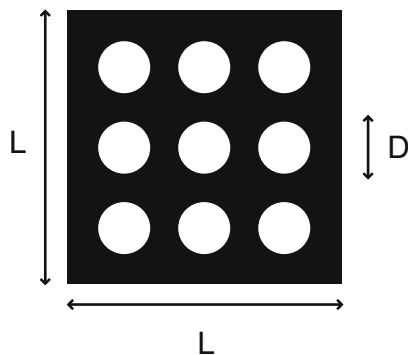
rehydrated the scaffolds by directly adding about 50  $\mu\text{L}$  of  $1\times$  PBS and cell media to the scaffolds, respectively.

### 2.3 Analysis of pore size

We visualized the scaffolds under phase contrast using a Zeiss Axiovert 40 equipped with an Axiocam MRC camera, and the software AxioVision. We used the software ImageJ to analyze the features of a three by three pore region of the collagen–GAG scaffolding. The size of the pore region was determined through the equation (which we derived through simple geometry):

$$L = \sqrt{\frac{\pi}{\text{VF}} \frac{3D}{2}},$$

where  $L$  is the distance of a side of a unit square surrounding a  $3\times 3$  matrix of pores,  $D$  is the diameter of a pore, and VF is the void fraction.



We segmented the black-and-white images by finding the edges (twice), and reduced the noise by maximizing the contrast and despeckling the images (twice). To maintain continuity in void and gel spaces, we eroded the images (twice) and then performed a Gaussian blur with a radius of 40 pixels. We then matched the features of the original cropped image by adjusting the threshold. We recorded ImageJ's summary analysis to determine the void fraction (defined by the area of void space over the total area in the unit square) and average pore diameter (among the nine pores). For each porous dimension, we analyzed three unit squares and averaged the results to yield a mean pore diameter and void fraction with one standard deviation distribution.

### 2.4 Assembly of multi-component structures

We aimed to mimic the interface between the basal lamina and dermis by layering a thin film of Matrigel on top of porous, hydrated collagen–GAG scaffolds. To recreate the basal lamina, we spread 30  $\mu\text{L}$  of chilled Matrigel (stock

concentration 8 mg/mL, BD Biosciences, Bedford MA) doped with 1- $\mu\text{m}$  diameter fluorescent red latex beads (Sigma, St. Louis MO) for purpose of visualization over a 35  $\mu\text{m}$  tall PDMS chamber (free of posts). We punched holes at the inlet and outlet to allow for fluid access. We then heated the gel to 37°C for 20 min to polymerize and crosslink fibers, and then flipped the stamps over, aligned and gently placed them on top of a hydrated microfabricated collagen–GAG scaffold with a designed mean pore size of 95  $\mu\text{m}$  and void porosity of 40%. We imaged the samples using an Olympus Fluoview 300 IX70 inverted confocal microscope (equipped with HeNe and Kr lasers at 488 and 568/647 nm excitation, 510 longpass filter, 550 shortpass filter, 605/645 and 700/775 bandpass filters, and scanning photomultiplier tube).

### 2.5 Cell migration studies

Using a multi-component structure, we studied the migration of fibroblasts from Matrigel through the microfabricated collagen–GAG scaffold. First, we spread Matrigel precursors at stock concentration over a 35  $\mu\text{m}$  tall PDMS chamber (free of posts), and gelled the mixture at 37°C for 20 min. We then stained 3T3-L1 fibroblasts (ATCC, Manassas VA) with CellTracker Orange CMRA (Molecular Probes, Carlsbad CA), and seeded them at a density of  $1.2\times 10^6$  cells/mL on the Matrigel slabs for 3 h. Next, we rehydrated a microfabricated collagen–GAG scaffold with an expected mean pore diameter of 120  $\mu\text{m}$  and a void fraction of 20% (sterilized under short wavelength UV for a few hours) on glass coverslips; we inverted this structure and placed the collagen–GAG portion against the cell-seeded Matrigel slabs (as a control, we also performed this procedure with a non-porous collagen–GAG scaffold). To visualize fibroblast migration through the collagen–GAG scaffolds over time, we used confocal microscopy (same equipment as above) to image the porous and non-porous collagen–GAG at bottom, middle and top of the composite structures at 3 h, 12 h, and 5 days post assembly. We kept the samples hydrated by saturating the air inside the dishes. We acquired and processed images in Fluoview.

## 3 Results

### 3.1 Microfabrication of collagen-based skin scaffolds with precise pore structures

We used computer-aided design and microfabrication to produce, with high spatial control, a thin layer of engineered scaffold containing dermal components such as collagen–GAG (which is prevalent in skin substitutes

(Schulz et al. 2000; Balasubramani et al. 2001; Jones et al. 2002)). Spatial control of porous features was previously identified as an important determinant for the rate of host tissue regeneration (Yannas et al. 1989; O'Brien et al. 2005). We sought to develop an alternative approach to precipitation or freeze-drying for fabricating collagen-based scaffolds that could allow for control of thickness and porous features, and serve as a basis for spatially precise bottom-up engineering of skin substitutes containing multiple cellular and extracellular components to promote healing.

We designed a microfabricated bioreactor inside which extracellular components and cell-encapsulated matrices are flowed through and gelled *in situ* (Fig. 1). The chamber contained regularly spaced cylindrical posts that corresponded to designed porous features for the scaffold. Similar in concept to micromolding in capillaries (MIMIC), the microreactor method was adapted specifically for production of skin-replacement scaffolds: the design was based on a millimeter- to centimeter-sized porous planar structure (rather than a series of channels or capillaries), the backing of the device was a flexible silicone elastomer layer (similar to the silastic backing in Integra), and the microreactor setup allowed sequential flowing and purging of different components before the gelling step (to facilitate the construction of spatially complex structures containing cells and extracellular matrix precursors).

### 3.2 Characterization of pore structures

First, we tested the ability of this method to fabricate collagen-based scaffolds of porous dimensions that are clinically relevant to skin replacements [Fig. 2(a)]. *In vivo*, two important spatial parameters were as critical as the scaffold degradation rate in determining the rate of tissue ingrowth (Yannas and Burke 1980; O'Brien et al. 2004, 2005): mean pore diameter (defined as the diameter of collagen-free pores; in our case, the average diameter of a 3×3 matrix of pores available for cell migration), and void

fraction (defined as the percentage of volume/area not occupied by collagen; in our case, the fraction of empty space over total area of a unit square encompassing a 3×3 matrix of pores). To set our initial boundaries of values of both parameters, we followed previous studies (Yannas et al. 1989) that found pores with mean sizes below 20 μm would not allow for free access to the fibrovascular cells, and pores with mean sizes greater than 125 μm would not allow for proper cell attachment (the optimal values in our design may be different because the geometries of the pores are different in this design from previous studies, see Discussion). We produced nine dehydrated scaffolds with different designed pore diameters and void fractions [Fig. 2(b)]. To measure the actual pore diameters and void fractions, we used the software ImageJ to analyze pore features in an automated and objective manner [Fig. 2(b)]. We found a ten-fold reduction in standard deviation of pore diameters from scaffolds produced using conventional lyophilization (±30 μm) to our method of microfabricated gel (±3–4 μm) for seven of the nine porous dimensions [Fig. 2(c)]. Eight of the nine dimensions met the designed pore diameters within the standard deviation, whereas only five of the nine dimensions met the designed void fraction within the standard deviation. Scaffolds with larger designed void fractions tended to yield lower actual values. Beyond the ranges shown in Fig. 2, we found that scaffolds containing void fractions higher than 70% or pore diameters smaller than 30 μm were difficult to produce (data not shown).

### 3.3 Handling of centimeter-long collagen-based skin scaffolds

A challenge of using thin layers of hydrogels (with Young's modulus of several thousand Pascals [Harada et al. 2007]) in clinical practice is to ensure ease of handling the scaffold. To confirm that a flexible silicone elastomer layer can be used as a backing for routine handling (similar to currently used dermal replacements [Schulz et al. 2000]),

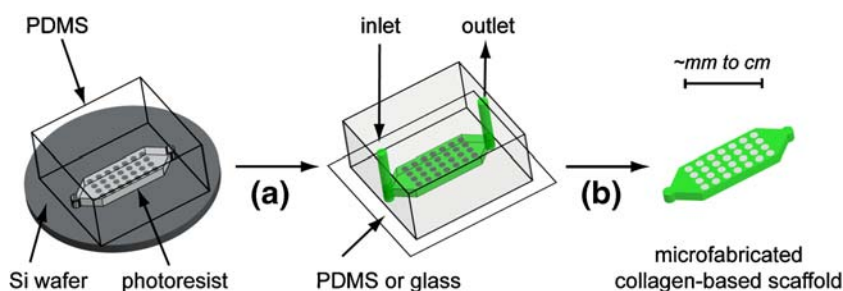


**Fig. 1** Schematic representation of the strategy for fabricating a porous collagen-GAG matrix. The end product is a large and thin microfabricated layer of hydrogel containing dermal components. (a) A porous pattern is transferred from photoresist features on a Si wafer to a PDMS mold, which is then conformally sealed on thin substrate

(either PDMS or glass). (b) Collagen-GAG precursors are injected into the microreactor and are first polymerized at 37°C before continued incubation at 37°C. Upon dehydration, the PDMS mold is carefully peeled to produce the collagen-based scaffold bearing the computer-designed pattern of pores

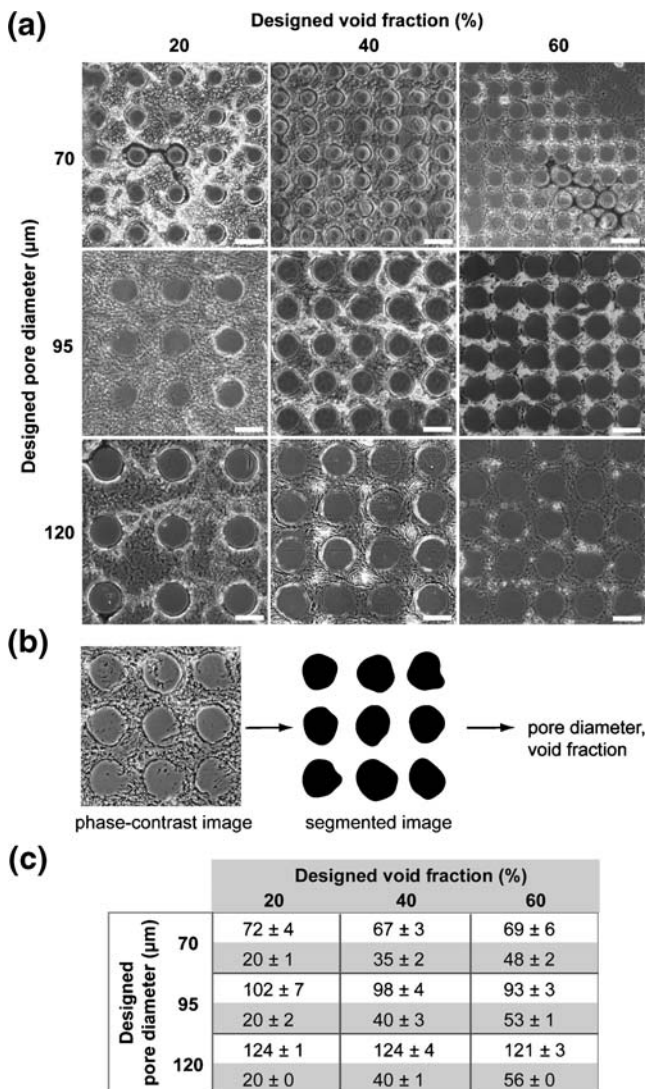


**Fig. 2** Microfabricated collagen-based scaffolds with a defined range of pore diameters and void fractions. **(a)** Phase-contrast images of nine dehydrated collagen and collagen–GAG scaffolds (after peeling off the PDMS top of the bioreactor) with different designed pore diameters and void fractions. Salt crystals formed in some locations, reflecting light intensely. *Scale bar* is 100 μm. **(b)** Determination of pore diameters and void fractions using an automated procedure for image analysis. Raw images are first segmented and then analyzed in ImageJ for actual pore diameters and porosities. **(c)** Table of mean pore diameter (*clear*) and void fraction (*shaded*) of scaffolds. Designed values are listed on the axes, and actual values with standard deviation are reported in the table

we microfabricated a 30 μm-thin and centimeter-long collagen–GAG structure (with designed pore diameter of 95 μm and void fraction of 40%) on top of a thin flexible PDMS membrane, and handled the structure using tweezers [Fig. 3(a)]. We were also able to carefully peel off some of the collagen layer from the backing [Fig. 3(b)]. This step required delicate handling to preserve the integrity of the scaffold, which tended to stick to the PDMS substrate. Lowly immunogenic, GAG serves to retard the breakdown

of collagen and increase the hydration, strength and elasticity of collagen. We chose chondroitin-6-sulfate, a repeating disaccharide of *N*-acetylgalactosamine and glucuronic acid, as a suitable GAG for several reasons: (1) it is used in skin scaffolds by Yannas and colleagues; (2) incorporation of 20% chondroitin-6-sulfate (v/v) increases collagen gel strength, with increases in Young's modulus, maximum load and stress at maximum load (Osborne et al. 1998); (3) addition of chondroitin-6-sulfate increases the growth rate of keratinocytes seeded on collagen gels (Hanthamrongwit et al. 1996; Osborne et al. 1997, 1999), and lyophilized collagen sponges (Burke et al. 1981; Yannas et al. 1982).

### 3.4 Precise pore structure to hasten cellular migration into skin substitutes

Next, using an *in vitro* assay, we directly tested the hypothesis that cellular migration is faster in a microfabricated porous collagen–GAG scaffold than a nonporous scaffold. Fast cellular migration into the grafted skin substitute is important because in skin-grafted areas of patients, the recruitment of mesenchymal (such as fibroblasts and endothelial cells) and epithelial cells from surrounding healthy dermal and subcutaneous tissues is necessary for tissue ingrowth as well as for drawing debrided wound margins together and establishing reepithelialization (Yannas and Burke 1980; Martin 1997; Schulz et al. 2000). We performed a cell migration assay by seeding fibroblasts onto a thin layer of Matrigel, and placing a 40 μm thick collagen–GAG scaffold (either containing microfabricated pores or without pores as a control)—backed by a silicone elastomer layer—on top (Fig. 4). While fibroblasts in the nonporous scaffold did not migrate from the Matrigel at the bottom through the collagen–GAG, fibroblasts migrated readily through the microfabricated porous collagen–GAG scaffold after 3 h [Fig. 4(a)]. Interestingly, fibroblasts localized near the pores at the collagen–Matrigel interface, but laterally dispersed as they migrated through the collagen–GAG; this migration behavior suggests the fibroblasts use the microfabricated pores as conduits for populating the collagen–GAG scaffold. 3D reconstructed images confirmed that the fibroblasts migrated through the porous scaffold after 3 h, and dispersed even further throughout the scaffold after 5 days [Fig. 4(b)].

### 3.5 Assembly of rationally engineered skin substitutes of higher structural complexity

Compared to collagen–GAG sponges, where cells migrate through gaps of tens of microns between collagen fibers, our porous microfabricated collagen–GAG scaffold features

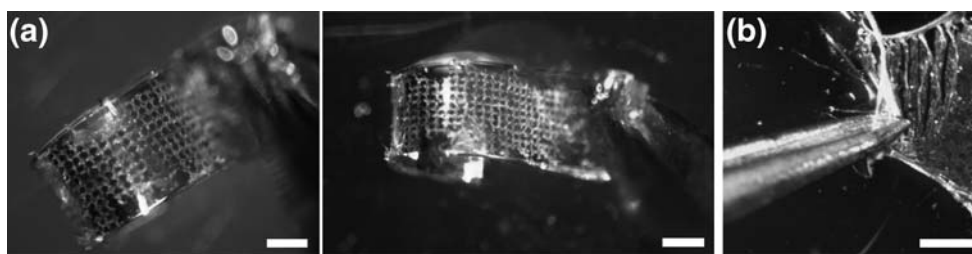


**Fig. 3** Large-scale fabrication and handling of collagen–GAG scaffolds. **(a)** Pictures of tweezers handling a centimeter-long collagen–GAG scaffold (dermal analog) resting on a thin PDMS membrane

(epidermal analog). *Scale bars* are 1 mm. **(b)** Picture of a collagen–GAG scaffold being released from a silicone elastomer backing using tweezers. *Scale bar* is 2 mm

two distinct regions: well-defined pores for cell migration, and extracellular matrix regions of natural collagen fibrous structure and density (hundreds of nanometers in pore size as in physiological dermis [Boron and Boulpaep 2005]). We further explored the potential of this microfabrication approach by adding additional skin components, in a step-wise manner, to the microfabricated porous collagen–GAG structure. Specifically, like the spatially distinct layers of natural skin [epidermis, basal lamina, and dermis; Fig. 5(a)], we laid a layer of Matrigel (which contains components from basal lamina) onto a microfabricated porous collagen-based layer. Also, we incorporated inlet

and outlet holes to a thin PDMS layer (that acts as a temporary epidermal analog) for possible controlled delivery of additional reagents [Fig. 5(b)]. A confocal image in the  $x$ – $z$  plane of this multi-component construct showed the intended spatial layering of collagen (which autofluoresces under confocal reflectance) and Matrigel with fluorescent cells encapsulated [Fig. 5(c), bottom left]. Further, a top-down fluorescence image in the  $x$ – $y$  plane of a porous microfabricated collagen–GAG scaffold with Matrigel containing fluorescent beads revealed three distinct regions as intended: pores (clear green), collagen fibers (dark green due to dense fibers), and fluorescent beads (red) in the Matrigel layer [Fig. 5(c), right].

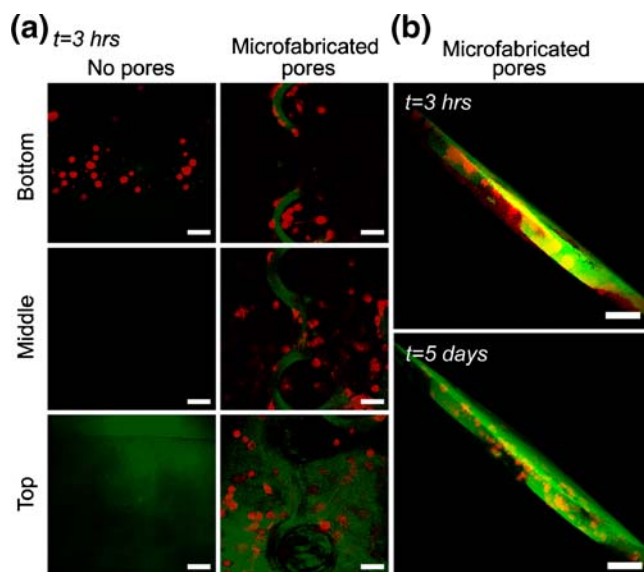


**Fig. 4** Fibroblast migration through microfabricated collagen–GAG scaffolds. Scaffolds (porous and non-porous) were placed on top of a fibroblast-seeded layer of Matrigel, and the migration of the fluorescent cells was tracked over 5 days. **(a)** Confocal fluorescence slices of *bottom* (interface of Matrigel with collagen–GAG), *middle* (collagen–GAG), and *top* (interface of collagen–GAG with PDMS) of the same composite structure. Two composite structures are shown: regular collagen–GAG scaffold as control (*left*), and porous collagen–GAG scaffold (*right*). Pictures were taken 3 h after assembly of composite structures. *Scale bars* are all 50  $\mu$ m. **(b)** 3D reconstructions of cell migration through porous collagen–GAG structures at 3 h and 5 days after assembly. *Scale bars* are all 50  $\mu$ m

## 4 Discussion

The microfabricated collagen–GAG scaffolds are structurally different from the collagen–GAG sponges produced by lyophilization: they contain two distinct regions of natural extracellular matrix and hollow pores. An advantage of this scaffold structure is that promotion of cell migration through the scaffold can be engineered independently of chemically modifying the native collagen structure. Specifically, the collagen region—which preserves the density of cell-attachment sites and fibrous structure of collagen fibers that affect the rate and mode of cell migration (Yannas and Burke 1980; O’Brien et al. 2005)—mimics the dermal extracellular matrix in terms of collagen concentration, composition, structure, and stiffness; this collagen region does not require chemical crosslinkers (such as glutaraldehyde, carbodiimides and diamines) or vacuum dehydration (which increases crosslink density via condensation or esterification reactions [Ratner 2004; Yannas 1972; Yannas et al. 1980]). With a natural collagen-based scaffold, the porosity of the microfabricated scaffold can be precisely fine-tuned to optimize the rate of cellular ingrowth (and hence tissue regeneration in the host upon grafting).

The distinct structure of the microfabricated scaffold brings up two issues not present for conventional collagen–GAG sponges: (1) Since the hollow cylindrical thru-pores

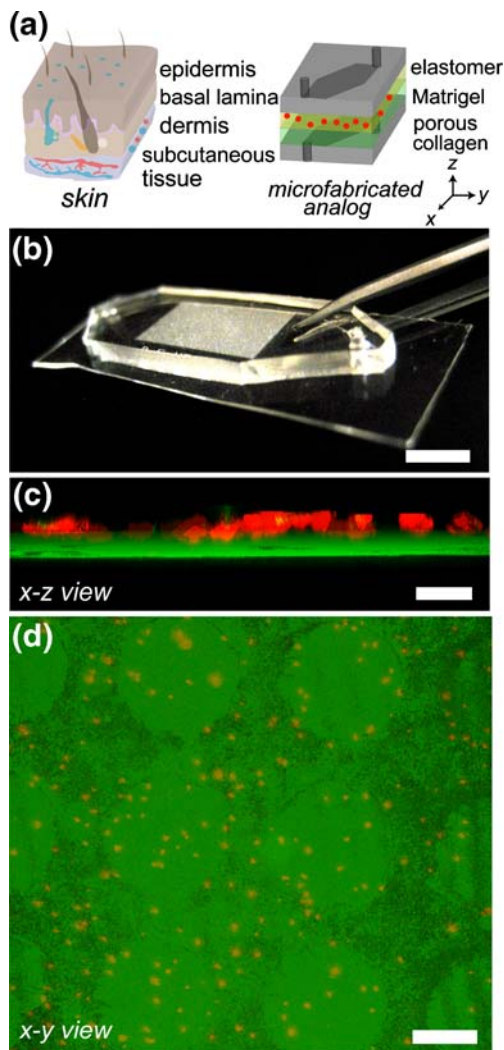


**Fig. 5** Microfabrication of multilayer structures for artificial skin. **(a)** (left) Schematic diagram of the layers of natural skin. (right) Schematic diagram of the layers of a microfabricated analog of skin. **(b)** Picture of overall multilayer structure, containing a PDMS stamp on top of a thin PDMS membrane for fabricating porous collagen–GAG scaffolds. Access to basal lamina is possible by punching holes through a stamp with open chamber, creating an inlet and outlet for reagent delivery (not shown). Scale bar is 5 mm. **(c)** Merged confocal fluorescence image ( $x$ – $z$  view) of microfabricated porous collagen–GAG (which autofluoresces as green under reflectance mode) and bulk Matrigel (with red fluorescent 3T3 fibroblasts seeded on top) sandwiched between two thin PDMS membranes. Scale bar is 50  $\mu$ m. **(d)** Merged confocal fluorescence image ( $x$ – $y$  view) of microfabricated porous collagen–GAG (dark green due to dense collagen fibers, with clear green pores due to high power set on the photomultiplier tube) and bulk Matrigel (embedded with 1- $\mu$ m diameter red fluorescent beads) sandwiched between two thin PDMS membranes. Scale bar is 50  $\mu$ m

are unlike the interconnecting pores of a 3D sponge (Yannas and Burke 1980; Yannas et al. 1980, 1989), would host cells readily attach to and migrate through the microfabricated scaffold? Based on our *in vitro* cellular migration studies, which suggest that the thru pores would likely serve as conduits for host cell repopulation (Fig. 4),

and on previous clinical skin grafting studies (Yannas et al. 1989; Schulz et al. 2000), we expect host remodeling will quickly fill the pores with native extracellular matrix. (2) Since the chondroitin-6-sulfate in the microfabricated scaffold is not wholly covalently attached to the collagen fibers, will it leach out of the scaffold? First, we believe that preservation of native extracellular matrix structure (in which collagen and GAG are not covalently cross-linked) may aid host regeneration. Also, some of the GAG may in fact be crosslinked to collagen fibers, since chondroitin-6-sulfate has previously been immobilized onto collagen fibers by condensation reactions via dehydration (between free carboxyl groups on glucuronic acid residues in the GAG chain with  $\epsilon$ -amino groups of lysyl residues in collagen), although the crosslinking is likely of a lesser degree in our method—due to residual hydration within collagen fibrils (Kopp et al. 1989; Leikin et al. 1997; Miles et al. 2002)—than previous studies (using high temperature vacuum dehydration, in which the elution of as much as 40% of the GAG originally coprecipitated with collagen was prevented [Yannas et al. 1980], and chemical treatment with carbodiimides [Hanthamrongwit et al. 1996] or glutaraldehyde [Yannas et al. 1980]).

As expected, the spatial fidelity of porous features is high in the microfabricated scaffold compared to lyophilization. For example, the microreactor technique exhibited about an order of magnitude improvement over lyophilized scaffolds (O'Brien et al. 2004) in terms of reproducibility (measured by standard deviation) in mean pore size and void fraction. Sources of error in lateral pore sizes included distortion of features from peeling off the PDMS mold, and most significantly, collagen contraction and variable structure after rehydration of the scaffold. Also, scaffolds with high void fractions were more difficult to fabricate than those with low void fractions. In the future, we believe the fidelity can be improved further by using the microreactor to reflow the channel with collagen precursors even after collagen contraction, or by directly patterning collagen–GAG composites in the presence of other biocompatible materials (e.g., polyethylene glycol hydrogels; Lee et al. 2006; Cheung et al. 2007). Although controllable, the thickness of the microfabricated construct was also compromised by collagen contraction, as we observed collapse of the collagen structure by up to two-fold due to dehydration. In future work, to mimic a full-thickness dermal layer (e.g. hundreds of microns), a thick photoresist layer can be spin-coated as a master; a thick and physically robust collagen–GAG scaffold may also facilitate peeling of the construct from the PDMS backing for surgical grafting.

The microreactor method is conceptually similar to micromolding in capillaries (MIMIC), but for producing skin scaffolds, it offers distinguishing features compared to

MIMIC and other soft lithographic techniques (such as replica molding and microtransfer molding; Tang et al. 2003, 2004): (1) Since it allows refilling of the microreactor volume, it can improve spatial fidelity of the features by pre-contracting the initially gelled collagen, and re-filling and re-gelling the void volume in the reactor (Tan and Desai 2004, 2005); (2) It is versatile for manufacturing multi-component systems because it readily allows the addition of cells and extracellular components to the scaffold; (3) It can be used to fabricate centimeter-scale planar porous scaffolds, rather than series of micrometer-scale channels, relevant to skin replacements. (4) Although collagen is the predominant extracellular matrix component in skin replacements, the microreactor can in principle be used for a diverse set of extracellular matrices, including those (such as alginate) that cross-link chemically rather than by temperature.

An important consideration in manufacturing micro-fabricated tissues is the cost and ease of scaling up production. The raw material cost of collagen and GAG needed to produce an 5 cm by 5 cm microfabricated scaffold is about \$0.16/cm<sup>2</sup>, which is comparable to Integra (whose market price is \$6.64/cm<sup>2</sup> (Jones et al. 2002)). The reusable microreactor does not add significantly to the cost of manufacturing, compared to gelling the mixture outside the device. In throughput, this method also compares favorably to freeze-drying techniques. For example, to manufacture a centimeter-sized scaffold, the procedure takes about 24 h, compared to 24 h for lyophilization and an additional 24 h for dehydrothermal crosslinking (O'Brien et al. 2004).

A goal of the manufacture of artificial skin is a construct that contains all the components of natural skin (including blood vessels, adnexal structures, and melanocytes); these constructs may decrease scarring in skin grafts, and serve as realistic skin models for a variety of *in vitro* testing [Fig. 5(a)]. The overall cellular and extracellular architecture of natural human epidermis and dermis is more complex than that of current skin substitutes. Current methods for multi-component fabrication of artificial skin have focused on pre-seeding of endothelial cells in the dermal region of the graft site (to accelerate formation of the vascular plexus), as well as delivery of genetically modified cells. Our work in this study has integrated fibroblasts, Matrigel, and a microfabricated biphasic collagen–GAG scaffold. As a microreactor, it can be integrated in the future with other high-throughput techniques we have developed on building composite structures (Cheung et al. 2007); we believe gelling *in situ* may be more versatile than other soft lithographic techniques that require a pre-mixing of components prior to formation of features.

Disadvantages of the approach in this study include a need for dehydrating the scaffold before peeling off the

PDMS (although this limitation also holds for lyophilized and dehydrothermally treated-collagen–GAG sponges, it poses a challenge for producing cell-encapsulated collagen regions), and the delicate handling required for thin hydrogel structures. Potential future directions include the construction of anatomically complex, biologically inspired scaffolds (Jeong et al. 2006), such as incorporation of growth factors (Baskaran et al. 2000; Ji et al. 2006; Cha and Falanga 2007), endothelial cells, or genetically modified skin cells to produce antibacterial protein (Vaikunth et al. 2006, 2007).

**Acknowledgments** We thank Jonathan Mansbridge for helpful advice on the project and manuscript, Alejandro-Rios Tovar for help with figures and photolithography, Allison Eng for exploratory research, Richard Harniman for photolithography training and hardware assistance at Columbia University's CEPSR Clean Room, Elizabeth Oswald for training on the confocal microscope, and members of the Sia Lab for reading the manuscript. We are grateful for funding provided by the Frank H. Buck Scholarship (C.D.C.) and a Scientist Development Grant from the American Heart Association (S.K.S.).

## References

- M. Balasubramani, T.R. Kumar, M. Babu, Burns **27**, 534 (2001)
- H. Baskaran, M.L. Yarmush, F. Berthiaume, J. Surg. Res. **93**, 88 (2000)
- E. Bell, B. Ivarsson, C. Merrill, Proc. Natl. Acad. Sci. USA **76**, 1274 (1979)
- E. Bell, H.P. Ehrlich, D.J. Buttle, T. Nakatsuji, Science **211**, 1052 (1981)
- W. Boron, E. Boulpaep, *Medical Physiology* (Saunders, Philadelphia, 2005)
- S.T. Boyce, G.D. Warden, Am. J. Surg. **183**, 445 (2002)
- J.F. Burke, I.V. Yannas, W.C. Quinby, C.C. Bondoc, W.K. Jung, Ann. Surg. **194**, 413 (1981)
- J.S. Cha, V. Falanga, Clin. Dermatol. **25**, 73 (2007)
- Y.K. Cheung, B.M. Gillette, M. Zhong, S. Ramcharan, S.K. Sia, Lab. Chip. **7**, 574 (2007)
- N. Dagalakis, J. Flink, P. Stasikelis, J.F. Burke, I.V. Yannas, J. Biomed. Mater. Res. **14**, 511 (1980)
- B.R. Downing, K. Cornwell, M. Toner, G.D. Pins, J. Biomed. Mater. Res. Part A **72A**, 47 (2005)
- M. Hanthamrongwit, W.H. Reid, M.H. Grant, Biomaterials **17**, 775 (1996)
- I. Harada, S.G. Kim, C.S. Cho, H. Kurosawa, T. Akaike, J. Biomed. Mater. Res. A **80**, 123 (2007)
- T. Jaksic, J.F. Burke, Annu. Rev. Med. **38**, 107 (1987)
- K.H. Jeong, J. Kim, L.P. Lee, Science **312**, 557 (2006)
- L. Ji, B.L. Allen-Hoffmann, J.J. De Pablo, S.P. Palecek, Tissue Eng. **12**, 665 (2006)
- I. Jones, L. Currie, R. Martin, Br. J. Plast. Surg. **55**, 185 (2002)
- J. Kopp, M. Bonnet, J.P. Renou, Matrix **9**, 443 (1989)
- H.J. Lee, J.S. Lee, T. Chansakul, C. Yu, J.H. Elisseeff, S.M. Yu, Biomaterials **27**, 5268 (2006)
- S. Leikin, V.A. Parsegian, W.H. Yang, G.E. Walrafen, Proc. Natl. Acad. Sci. USA **94**, 11312 (1997)
- S. MacNeil, Nature **445**, 874 (2007)
- P. Martin, Science **276**, 75 (1997)

- C.A. Miles, T.J. Sims, N.P. Camacho, A.J. Bailey, *J. Mol. Biol.* **321**, 797 (2002)
- J. Morgan, R. Sheridan, R. Tompkins, M. Yarmush, J. Burke, ed. by B. Ratner. *Burn Dressings and Skin Substitutes* (Academic, San Diego, 2004)
- F.J. O'Brien, B.A. Harley, I.V. Yannas, L. Gibson, *Biomaterials* **25**, 1077 (2004)
- F.J. O'Brien, B.A. Harley, I.V. Yannas, L.J. Gibson, *Biomaterials* **26**, 433 (2005)
- C.S. Osborne, W.H. Reid, M.H. Grant, *J. Mater. Sci. Mater. Med.* **8**, 179 (1997)
- C.S. Osborne, J.C. Barbenel, D. Smith, M. Savakis, M.H. Grant, *Med. Biol. Eng. Comput.* **36**, 129 (1998)
- C.S. Osborne, W.H. Reid, M.H. Grant, *Biomaterials* **20**, 283 (1999)
- G.D. Pins, M. Toner, J.R. Morgan, *FASEB J.* **14**, 593 (2000)
- B. Ratner, *Biomaterials Science: An Introduction to Materials in Medicine*, 2nd edn. (Academic, New York, 2004)
- J.T. Schulz 3rd, R.G. Tompkins, J.F. Burke, *Annu. Rev. Med.* **51**, 231 (2000)
- S.K. Sia, G.M. Whitesides, *Electrophoresis* **24**, 3563 (2003)
- D.M. Supp, S.T. Boyce, *Clin. Dermatol.* **23**, 403 (2005)
- W. Tan, T.A. Desai, *Biomaterials* **25**, 1355 (2004)
- W. Tan, T.A. Desai, *J. Biomed. Mater. Res. A* **72**, 146 (2005)
- M.D. Tang, A.P. Golden, J. Tien, *J. Am. Chem. Soc.* **125**, 12988 (2003)
- M.D. Tang, A.P. Golden, J. Tien, *Adv. Mater.* **16**, 1345 (2004)
- S.S. Vaikunth, M. Marwan, J. Parvadia, M. Ripberger, B. Kalinowska, E. Uzvolgy, A. Supp, D. Alae, S. Boyce, T. Crombleholme, D. Supp, *J. Am. Coll. Surg.* **203**, S61 (2006)
- S.S. Vaikunth, J. Parvadia, A.R. Maldonado, B. Kalinowska, M. Ripberger, A. Supp, S.T. Boyce, T.M. Crombleholme, D. Supp, *Wound Repair Regen.* **15**, A22 (2007)
- P. Waymack, R.G. Duff, M. Sabolinski, *Burns* **26**, 609 (2000)
- L.M. Wilkins, S.R. Watson, S.J. Prosky, S.F. Meunier, N.L. Parenteau, *Biotechnol. Bioeng.* **43**, 747 (1994)
- I.V. Yannas, *J. Macromol. Sci. Rev. Macromol. Chem. Phys.* **C7**, 49 (1972)
- I.V. Yannas, J.F. Burke, *J. Biomed. Mater. Res.* **14**, 65 (1980)
- I.V. Yannas, J.F. Burke, P.L. Gordon, C. Huang, R.H. Rubenstein, *J. Biomed. Mater. Res.* **14**, 107 (1980)
- I.V. Yannas, J.F. Burke, D.P. Orgill, E.M. Skrabut, *Science* **215**, 174 (1982)
- I.V. Yannas, E. Lee, D.P. Orgill, E.M. Skrabut, G.F. Murphy, *Proc. Natl. Acad. Sci. USA* **86**, 933 (1989)